

Phase diagrams of nanoparticles of diluted magnetic semiconductors

M. Hamedoun^(a,*), R. Masrour^(a), K. Bouslykhane^(a), A. Hourmatallah^(a, b), N. Benzakour^(a) and A. Benyoussef^(c)

a: Laboratoire de Physique du Solide, Université Sidi Mohammed Ben Abdellah, Faculté des sciences, BP 1796, Fes, Morocco.

b: Equipe de Physique du Solide, Ecole Normale Supérieure, BP 5206, Bensouda, Fes, Morocco.

c: LMPHE, Faculté des Sciences, Université Mohamed V, Rabat, Morocco

* Corresponding author: e-mail: hamedoun@hotmail.com

The magnetic properties of diluted magnetic semi conductors (DMS) $Cd_{1-x}Mn_xTe$ are investigated. Using the mean field theory, we have evaluated the critical temperature from the nearest neighbour interactions and the energy exchange for the different diameter of the $Cd_{0.5}Mn_{0.5}Te$ nanoparticle. The critical exponents are obtained. The magnetic phase diagrams (T_c versus dilution x) have been determined by the High-temperature series expansions. The critical exponents associated with the magnetic susceptibility (γ) and correlation lengths (ν) are deduced.

Keywords: Diluted magnetic semi conductors; critical temperature; nanoparticle; critical exponents; High-temperature series expansions; Padé approximants, Phase diagram.

1-Introduction

Diluted magnetic semiconductors (DMS, known also as semimagnetic semiconductors) are compounds based on typical semiconductors (like $CdTe$ or $InAs$), for which a fraction of nonmagnetic cations has been replaced by magnetic ions (typically transition metal ions like Mn , Fe or rare earth metal ions) [1] DMS bridge the physics of semiconductors and magnetic since they show typical semiconductor behaviour and they also reveal pronounced magnetic properties. $Cd_{1-x}Mn_xTe$, Zinc-blende structure DMS alloys are the most typical representative of DMS. They can be considered as mixed crystal systems between two Zinc-blende phase materials, $CdTe$ ($ZnTe$) and $MnTe$. In particular magnetism of these materials is typical for magnetic ions possessing a spin momentum $S = \frac{5}{2}$, which would correspond to Mn^{2+} (d^5) centers. Several magnetic phases could be observed in such materials, whose appearance depends on the magnetic ion concentration and temperature range [2-4]. The magnetic phase diagrams of the above two systems consist of two regions: a high-temperature, paramagnetic phase and low temperature frozen phase. The latter phase generally occurs when $x > 0.2$, but recent works has shown that spin freezing can also occurs for

lower values of x at very low temperature [5,6]. For highest magnetic concentration, a gradual transition between SG and AFM phases has been observed [3]. The pure system $MnTe$ presents a truly long-range, type III AFM ordering [7].

We have used the mean field theory, for calculated the critical temperature from the nearest neighbour J_1 [8] interactions and the energy exchange for the different diameter of the $Cd_{0.5}Mn_{0.5}Te$ nanoparticle. This shifts of the critical temperatures $T_c(D)$ from the bulk

value $\left[\frac{T_c(\infty)}{T_c(D)} - 1 \right]$ can be described by a power

law $D^{-\lambda}$, where λ is the inverse of the correlation length exponent. Another part of this paper concerns the interesting topic of magnetic structure and spin glass behaviour in the diluted magnetic semiconductors $Cd_{1-x}Mn_xTe$ with $0 \leq x \leq 1$. The Padé approximant (P.A) [9] analysis of the high-temperature series expansion (HTSE) of the correlation length has been shown to be a useful method for the study of the critical region [10,11]. We have used this technique to determine the phase diagrams and the critical exponents γ and ν associated with the

magnetic susceptibility χ and the correlation length in the range $0 \leq x \leq 1$.

II. Critical temperatures and critical exponent's calculations

Starting with the well known Heisenberg model, the Hamiltonian of the system is given by:

$$H = -2 \sum_{i,j} J_{ij} \vec{S}_i \vec{S}_j \quad (1)$$

Where, J_{ij} is the exchange integral between the spins situated at sites i and j . \vec{S}_i is the spin operator localised at the site i . In this work we consider the nearest neighbour (nn) and next nearest neighbour (nnn) interactions J_1 and J_2 respectively.

$$H = J_1 \sum_{i,j} \vec{S}_i \vec{S}_j - J_2 \sum_{i,k} \vec{S}_i \vec{S}_k \quad (2)$$

The sums over ij and ik include all (nn) and (nnn) pair interactions, respectively. The mean field approximation leads to a simple relations between the critical temperature T_c , respectively, and the considered one exchange integral J_1 .

Following, the method of Holland and Brown [12], the expression of T_c is:

$$T_c = \frac{2}{3K_B} S(S+1) [zJ_1] \quad (3)$$

Where K_B is the Boltzmann constant, $z = 12$ and $S = \frac{5}{2}$.

Using the experimental values $J_1(D)$ obtained by magnetic measurement [13] for the $Cd_{0.5}Mn_{0.5}Te$ nanoparticle. We have deduced the values of critical temperature T_c . From these values, we have derived the energy exchange, for different diameter of nanoparticle. These results are given in table 1. The temperature shift has been observed in numerous experimental studies and it has also been investigated in theory [13-17].

$D(nm)$	$-\frac{J_1}{K_B}(K)$ [8]	$T_c(K)$	$-\frac{E}{S^2}(K)$
bulk	8.1	18.90	97,12
8.0	7.8	18.20	93,6
7.2	6.9	16.10	82,72
6.7	8.9	20.76	106,72

Table 1: The critical temperature $T_c(K)$, the first exchange integrals and the energy of $Cd_{0.5}Mn_{0.5}Te$.

Specifically, the critical temperature T_c must be regarded as a diameter-dependent parameter,

$T_c(D)$ which approaches the bulk critical temperature $T_c(\infty)$ as the scale factor L (the diameter of nanoparticle) approach ∞ . It has been shown that the approach of $T_c(D)$ to $T_c(\infty)$ can also be described by a simple power law [18] characterized by a shift exponent λ defined by:

$$1 - \frac{T_c(D)}{T_c(\infty)} \propto D^{-\lambda} \quad (4)$$

The shift exponent λ is given by $\lambda = \frac{1}{\nu_b}$

where ν_b is the correlation length critical exponent.

In Fig. 1, we exhibit the dependence of the shift $\delta T = \frac{T_c(\infty) - T_c(D)}{T_c(D)}$ whit $D(nm)$ in a Log-Log scale to determine the exponent λ by using equation (4) for Heisenberg model. The obtained values of nanoparticle is $\nu_b = 1.1 \pm 0.1$. This value is qualitative accordance with the universality class hypothesis [19].

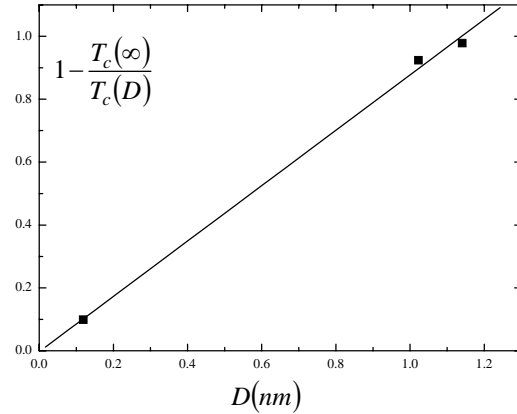


Fig. 1: Log-log plot of the shift of reduced critical temperature $1 - \frac{T_c(\infty)}{T_c(D)}$ versus diameter $D(nm)$ of $Cd_{0.5}Mn_{0.5}Te$ nanoparticle.

III. High-temperature series expansions

In this section we shall derive the high-temperature series expansions (HTSE) for both the zero field magnetic susceptibility χ to order six in β . The relation ship between the magnetic susceptibility per spin and the correlation functions may be expressed as follows:

$$\chi(T) = \frac{\beta}{N} \sum_{ij} \langle \vec{S}_i \vec{S}_j \rangle \quad (5)$$

Where $\beta = \frac{1}{k_B T}$ and N is the number of magnetic

$$\text{ion. } \langle S_i S_j \rangle = \frac{\text{Tr} S_i S_j e^{-\beta H}}{\text{Tr} e^{-\beta H}} \text{ is the correlation}$$

function between spins at sites i and j . The expansion of this function in powers of β is

$$\text{obtained as follows [20]: } \langle \vec{S}_i \vec{S}_j \rangle = \sum_{l=0}^{\infty} \frac{(-1)^l}{l!} \alpha_l \beta^l \quad (6)$$

$$\text{with: } \alpha_l = \nu_l - \sum_{k=0}^{l-1} C_k^l \alpha_k \mu_{l-k},$$

$$\nu_m = \langle \vec{S}_i \vec{S}_j H^m \rangle_{T=\infty} \text{ and } \mu_m = \langle H^m \rangle_{T=\infty}$$

The calculation of the coefficients α_l leads to a diagrammatic representation [21], which involves two separate phases:

(a) The finding and cataloguing of all diagrams or graphs which can be constructed from one dashed line connecting the site i and j , and l straight lines, and the determination of diagrams whose contribution is nonvanishing. This step has already been accomplished in the Stanley work.

(b) Counting the number of times that each diagram can occur in the magnetic system.

In our case, we have to deal with nearest-neighbour coupling J_{ij} . The coefficient α_l may be expressed for each topological graph as [20]:

$$\alpha_l = \bar{S}^2 (-2\bar{S}^2)^l (J_{ik_1}^{m_1} J_{k_2 k_3}^{m_2} \dots J_{k_w j}^{m_w}) [\alpha_l] \quad (7)$$

with the condition $\sum_{r=1}^w m_r = l$

for $m_r = 0, 1, \dots, l$. The ‘‘weight’’ $[\alpha_l]$ of each graph is tabulated and given in Ref. [22] and k_1, k_2, \dots, k_w represent the sites surrounding the sites i and j . In an early [20] work, the coefficient

α_l required for the calculation of the three first correlation functions in the case of the FCC lattice are given. In [11], a relation between the susceptibility, correlation length and the three first correlation functions is given in the case face centred cubic lattice with a particular ordering vector $Q = (0, 0, k)$. In the ferromagnetic case we get $k = 0$. The high temperature series expansion of $\chi(T)$ gives the function:

$$\chi(T) = \sum_{m=-n}^n \sum_{n=1}^6 a(m, n) y^m \tau^n \quad (8)$$

The high temperature series expansion of ξ^2 gives the function:

$$\xi^2(T) = \sum_{m=-n}^n \sum_{n=1}^6 b(m, n) y^m \tau^n \quad (9)$$

Where $y = \frac{J_2}{J_1}$ and $\tau = \frac{2S(S+1)J_1}{k_B T}$. The values of exchange interactions used are $J_1 = -13K_B$ and

$J_2 = -4K_B$ given in [23]. The series coefficients $a(m, n)$ and $b(m, n)$ are given in [24]. In spin-glasses (S.G) critical behaviour near the T_{SG} SG transition, it is expected not in the linear part χ_0 of the dc susceptibility χ , but in the nonlinear susceptibility $\chi_s = \chi - \chi_0$. This is due to the fact that the order parameter q in the spin glass state is not the magnetization but the quantity $q = \frac{1}{N} \sum_i \langle S_i^2 \rangle_{av}$. As suggested by Edwards and Anderson [25], leading to an associated susceptibility $\chi_s = \frac{1}{NT^3} \sum_{ij} \left[\langle S_i S_j \rangle^2 \right]_{av}$, where the correlation length of the correlation function $\left[\langle S_i S_j \rangle^2 \right]$ possibly diverges at

$T = T_{SG}$. The behaviour of the nonlinear susceptibility has been already extensively studied theoretically and experimentally [26, 27]. We have used the expression of χ_s , to determinate the critical temperature in the region of spin glass for DMS $Cd_{1-x}Mn_xTe$. Figure 2 show magnetic phase diagram of DMS $Cd_{1-x}Mn_xTe$ nanoparticle. We can see the good agreement between the magnetic phase diagrams obtained by the HTSE technique and the experimental ones, in particular in the case of the last systems of which the phase diagrams have been established well by different methods [28-29]. The results given by the HTSE method are comparable with the experimental points that the results deals by the replica method [30].

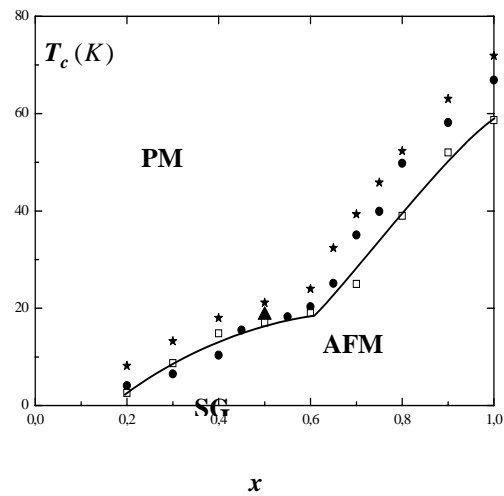


Fig. 2: The magnetic phase diagram of $Cd_{1-x}Mn_xTe$. The various phases are the paramagnetic phase (PM), antiferromagnetic

phase (AFM) ($0.6 \leq x \leq 1$), and the spin glass phase (SG) ($0.2 \leq x \leq 0.6$). The open squares are the theoretical results. The solid circle, the up triangle solid, the solid star represent the experimental points deduced by measurements magnetic and the by replica method [32], [8] and [30], respectively.

The simplest assumption that one can make concerning the nature of the singularity of the magnetic susceptibility $\chi(T)$ is that at the neighbourhood of the critical point the above two functions exhibit an asymptotic behaviour:

$$\chi(T) \propto (T - T_c)^{-\gamma} \quad (10)$$

$$\xi^2(T) \propto (T_c - T)^{-2\nu} \quad (11)$$

Estimates of T_c and γ for $Cd_{1-x}Mn_xTe$ have been obtained using the Padé approximate method (P.A) [9] in the range $0 \leq x \leq 1$. The simple pole corresponds to T_c and the residues to the critical exponents γ and ν . The obtained central values are $\gamma = 1.4 \pm 0.1$ and $\nu = 0.9 \pm 0.1$. These values are nearest of the Heisenberg model.

IV. Discussion and conclusion

We have used the experimental value of $J_1(x=0.5)$ [8] to derive the critical temperature T_c and the energy exchange of the magnetic structure for different diameter of $Cd_{0.5}Mn_{0.5}Te$ nanoparticle. These results are given in table 1. The critical temperature versus of the different diameter of $Cd_{0.5}Mn_{0.5}Te$ nanoparticle is given in table 1. In this table the critical temperature decreases with the number of diameter. On the other hand, according to the universality hypothesis, critical phenomena can be described by quantities that do not depend on the microscopic details of the system, but only on global properties such as the dimensionality and the symmetry of the order parameter. It has been a point of interest to see the influence of exchange coupling on the behavior of the critical exponent

$\nu_b = \frac{1}{\lambda}$ associated with the magnetic

References

- [1] See for example, Semiconductors and Semimetals, 25, *Diluted Magnetic Semiconductors*, eds. J. K. Furdyna and J. Kossut, (Academic Press 1988); *Semimagnetic Semiconductors and Diluted Magnetic Semiconductors*, eds. M. Balkanski and Averous (Plenum Press 1991); J. Kossut and W. Dobrowolski, in *Handbook of Magnetic Materials*, ed. K. H. Bushow, 7, 231 (North Holland, Amsterdam 1993).
- [2] S. P. Mcalister, J. K. Furdyna, And W. Giritat, Phys. Rev. B **29**, (1984) 1310.

$$1 - \frac{T_c(D)}{T_c(\infty)} \propto D^{-\lambda}, \quad \text{of the } Cd_{0.5}Mn_{0.5}Te$$

nanoparticle. These values are nearest of the Heisenberg model. The high-temperature series expansion (HTSE) extrapolated with Padé approximants method is shown to be a convenient method to provide valid estimations of the critical temperatures for real system. By applying this method to the magnetic susceptibility $\chi(T)$ we have estimated the critical temperature T_c for each dilution x . The obtained magnetic phase diagram of the DMS $Cd_{1-x}Mn_xTe$ system is presented in figure.2. Several thermodynamic phases may appear including the paramagnetic (PM), Antiferromagnetic (AFM) $0.6 \leq x \leq 1$ and spin-glass (SG) phase in range $0 \leq x \leq 0.6$. The percolation threshold obtained $x_c \approx 0.2$, is the critical concentration for the appearance of an infinite percolative cluster produced by the first nn hops only. This value is comparable with $x_c = 0.19$ obtained by [31]. In this figure we have included, for comparison, the experimental results obtained by magnetic measurement. From this figure one can see good agreement between the theoretical phase diagram and experimental results. In addition, we have determined the region spin glaze while using the expression of the nonlinear susceptibility. In the other hand, the value of critical exponents γ associated to the magnetic susceptibility $\chi(T)$, have been estimated in the range of the composition $0 \leq x \leq 1$. The sequence of [M, N] PA to series of $\chi(T)$ has been evaluated. By examining the behaviour of these PA, the convergence was found to be quite rapid. Estimates of the critical exponents associated with susceptibility and correlation length are found to be $\gamma = 1.4 \pm 0.1$ and $\nu = 0.9 \pm 0.1$. These values are insensitive to dilution x . These values are nearest of the Heisenberg model.

- [3] S. Oseroff and F. G. Gandra, J. Appl. Phys. **57**, (1985) 3421.
- [4] A. Twardowski, Phys. Scr, T **39**, (1991) 124.
- [5] D. Karaoulanis, J. P. Xanthakis and N. C. Bacalis. J. Magn. Magn. Mater. **221**, (2000) 407, D. Karaoulanis, J. P. Xanthakis and C. Papatrian tafillon, J. Magn. Magn. Mater. **161**, (1996) 231.
- [6] M. A. Novak, O. G. S&ymko, D. J. Zheng and S. Oseroff, Physica (b) **126**, (1984) 469.

- [7] K. Ando, K. Takahashi, and T. Okuda. Phys. Rev. B **46**, (1992) 12289, J. Diouri, J. P. Lascaray, and M. El Amrani, Phys. Rev. B **31**, (1985) 7995.
- [8] C. H. Power, O. Contreras, E. Calderón, J.C. Chervin, E. Snoeck, J.M. Broto, Alfa Meeting Highfield Vienne 26th to 30th April 2004.
- [9] “*Padé Approximants*”, edited by G. A. Baker and P. Graves-Morris (Addison-Wesley, London, 1981).
- [10] R. Navaro, Magnetic Properties of Layered Transition Metal Compounds, Ed. L.J.DE Jongsgh, Darenta: Kluwer 1990 (p.105).
- [11] M. C. Moron, J. Phys: Condensed Matter **8** (1996) 11141.
- [12] W. E. Holland and H. A. Brown, Phys-Stat. Sol (a) **10** (1972) 249.
- [13] Ou J T, Wang F and Lin D L, Phys. Rev. B **56** (1997) 2805.
- [14] Henkel M, Andrieu S, Bauer P and Piecuch M, Phys. Rev. Lett. **80** (1998) 4783.
- [15] A. Saber, A. Ainane , F. Dujardin , N. El Aouad , M. Saber M and B. Stébé, J. Phys.: Condens. Matter **12** (2000) 43.
- [16] R. Zhang and R. F.Wills Phys. Rev. Lett. **86** (2001) 2665.
- [17] J. Cabral Neta , J. Ricardo de SousaJ and J. A. Plascak, Phys. Rev. B **66** (2002) 064417.
- [18] C. Domb, J. Phys. A **6** (1973) 1296.
- [19] Kok-Kwei Pan, Phys. Rev. **71**, (2005) 134524.
- [20] H. E. Stanley and T. A. Kaplan, Phys. Rev. Lett. **16**, (1966) 981.
- [21] M. Hamedoun, M. Houssa, N. Benzakour, and A. Hourmatallah, J. Phys: Condens. Mater. **10**, (1998) 3611.
- [22] M. Hamedoun, M. Hachimi, A. Hourmatallah and K. Afif, J. Magn. Magn. Mater **283** (2001) 290-295.
- [23] B. E. Larson, K. C. Hass, R. L. Aggarwal, Phys. Rev. B, **33** (1986) 1789.
- [24] N. Benzakour M. Hamedoun, M. Houssa, A. Hourmatallah, and F. Mahjoubi, Phys. Stat. Sol. (b) **212** (1999) 335.
- [25] S. F. Edwards and P. W. Anderson, J. Phys. F **5**, (1975) 965.
- [26] S. Katsura, Prog, Theo. Phys. **55**, (1976) 1049.
- [27] G. Toulouse and M. Gabay, J. Phys. Lett. **42**, (1981) L 103
- [28] M. Alba, Hammann and M. Nougues, J. Phys, C **15** (1982) 5441.
- [29] K. Afif, A. Benyoussef, M. Hamedoun and A. Hourmatallah, Phys. Stat. Sol (b) **219** (2000) 383.
- [30] M. Hamedoun, Z. El Achheb, H. Bakrim, A. Hourmatallah, N. Benzakour, and A. Jorio, Phys. Stat. Sol. **236**, (2003) 661.
- [31] N. Samarth, J. K. Furdyna, Proc. IEEE, **78** (6), (1990) 990.
- [32] A. Stachow-Wojcik, W. Mac, A. Twardowski, G. Karczzewski, E. Janik, T. Wojtowicz, J. Kossut and E. Dynowska, Phys. Stat. Sol (a) **177**, (2000) 555.